

ELECTRONIC SUPPLEMENTARY MATERIAL

Hydrogen-bond-assisted topochemical synthesis of a multivalent zwitterionic tetramer via concomitant cross- and homo [2+2] photocycloadditions. Theoretical antiviral activity against SARS-CoV-2.

Ana M. Escalona,^a Frank W. Heinemann^b, Alexander Briceño^{a*}, Ysaías J. Alvarado^c, José Luis Paz^d, Carla Lossada^e, Lenin González-Paz^{e*}, Robert A. Toro^f and José Antonio Henao^f.

^aInstituto Venezolano de Investigaciones Científicas (IVIC), Centro de Química. Laboratorio de Síntesis y Caracterización de Nuevos Materiales. Caracas 1020-A, Venezuela.

^bFriedrich-Alexander-Universität Erlangen-Nürnberg (FAU), Department of Chemistry and Pharmacy, Inorganic Chemistry. D-91058 Erlangen, Germany.

^cIVIC, Centro de Biomedicina Molecular, Laboratorio de Química Biofísica Teórica y Experimental. Maracaibo, Zulia, Venezuela.

^dUniversidad Nacional Mayor de San Marcos, Facultad de Química e Ingeniería Química, Departamento Académico de Química Inorgánica. Lima, Perú.

^eIVIC, Centro de Biomedicina Molecular, Laboratorio de Biocomputación. Maracaibo, Zulia, Venezuela.

^fUniversidad Industrial de Santander (UIS). Laboratorio de Rayos X Parque Tecnológico Guatiguará, Piedecuesta, Bucaramanga, Colombia.

Table of Contents

1. Experimental section	2
2. Elemental analyses	4
3. NMR spectra	7
4. FT-IR spectra	9
5. ESI-MASS spectrum	10
6. Crystal structures	11
7. Biophysical-Computational characterization	15

1. Experimental section

General considerations

All reagents were obtained from commercial sources and used without further purification. The elemental analyses were performed on a EA1108 CHNS-O Fison analyzer. The FT-IR spectra were recorded from KBr discs, using Nicolet Magna-IR 560 or Perkin-Elmer RX1 1605 spectrometers. NMR spectra were recorded on Bruker Avance AM 300 or 500 MHz spectrometers in DMSO- d_6 . EI-MS analyses were performed on a Thermo Finnigan mass spectrometer with Triple Quadrupole and electrospray ionization (ESI). For the irradiation of the samples a BLACKRAY UVP 100W B100A UV lamp was used.

Synthesis of (3-H₂PA⁺)·(HCda⁻)·2H₂O (1): Under stirring, a solution of *trans*-3-(3-pyridyl)acrylic acid (200 mg, 1.34 mmol) in 10 mL of methanol was added to 30 mL of a methanolic solution of chelidonic acid (247 mg, 1.34 mmol). Slow evaporation of the resulting solution at room temperature yielded 360 mg (73%) of pink rhombohedral diffraction-quality single crystals. Elemental Analysis (%): Calculated for C₁₅H₁₅O₁₀N: C, 48.79; H, 4.09; N, 3.79. Found: C, 48.80; H, 4.05; N, 3.76. FT-IR (KBr, cm⁻¹): ν (O-H): 3545 and 3358, ν (=C-H): 3100-3068, ν (C=C): 1597 and 1461, ν (COO⁻): 1647 and 1401, ν (N⁺-H): 2470, ν (C=O): 1647, ν (C-O-C): 1288 and 1183, ν (=C-H): 784 and 706, ν (O-H): 3220-2570, ν (C=O): 1710, ν (C-O): 1270. ¹H RMN (300 MHz, DMSO- d_6), δ (ppm): 8.84 (d, J = 1.56 Hz, 1H), 8.57 (dd, J = 4.74 Hz, 1.23 Hz, 1H), 8.16 (ddd, J = 1.77 Hz, 1H), 7.61 (d, J = 16.15 Hz, 1H), 7.44 (dd, J = 7.92 Hz, 4.74 Hz, 1H), 6.94 (s, 2H), 6.68 (d, J = 16.12 Hz, 1H).

Solid state reactivity: crystals or a powdered crystalline sample (17 mg) of **1** were placed in Pyrex glass capsules and irradiated with a UV lamp at 350 nm for 5 days. During this period, the samples were mixed every 3 h to ensure uniform irradiation. In the case of the powdered sample, it was mechanically re-ground during 15-30 min with some drops of methanol each time and then irradiated. Both, the crystal and powdered samples, turned orange upon irradiation. The crystals presented multiple fractures that prevented X-ray diffraction analysis. At the end of the irradiation period, the powdered sample was washed by stirring in hot methanol for 30 min and then filtered to get compound **2** as a beige solid. Yield: (14 mg, 86%). Crystallisation of **2** from dry DMSO gave single crystals suitable for X-ray diffraction analysis. Elemental analysis (%): Calculated for C₃₀H₂₈O₁₉N₂: C, 50.01; H, 3.92; N,

3.88. Found: C, 49.79; H, 3.86; N, 4.14. FT-IR (KBr, cm^{-1}): $\nu(\text{O-H})$: 3428, $\nu(=\text{C-H})$: 3102-3066, $\nu(\text{C=C})$: 1600, 1544 and 1468, $\nu(\text{COO}^-)$: 1626 and 1404, $\nu(\text{N}^+\text{-H})$: 2954-2340, $\nu(\text{C=O})$: 1626, $\nu(\text{C-O-C})$: 1172, $\nu(=\text{C-H})$: 832, $\nu(\text{O-H})$: 3450-2500, $\nu(\text{C=O})$: 1708, $\nu(\text{C-O})$: 1268. EM (m/z): 667.07 $[\text{M}+\text{H}]^+$. ^1H RMN (300 MHz, DMSO-d_6), δ (ppm): 8.50 (s, 2H), 8.46 (d, $J = 3.90$ Hz, 2H), 7.68 (d, $J = 7.57$ Hz, 2H) 7.37 (dd, $J = 7.32$ Hz, 4.86 Hz, 2H), 4.25 (d, $J = 9.07$ Hz, 2H), 3.82 (s, 2H), 3.66 (t, $J = 10.23$ Hz, 2H), 3.55 (d, $J = 10.51$ Hz, 2H).

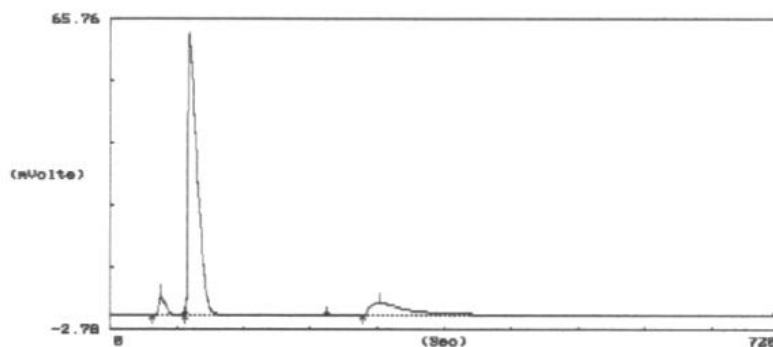


Figure S1. Crystals of assembly **1** (a) before irradiation and (b) after irradiation. (c) Isolated photoproduct **2**.

2.-Elemental analysis of assembly 1:

EAGER 200 Stripchart

Sample Ident. : 32 MEB-43 Filename : ag30506



EAGER 200 Peak Integration Report

Instrument name : Instrument #1 Bline drift (μV):-.7
 Company Name : IVIC Operator Ident. : E.S.
 Sample Ident. : 32 MEB-43 Filename : ag30506
 Sample Weight : 2.053 Calc.method: using 'K. Factors'

No. (#)	Type (#)	Start (Sec)	End (Sec)	Ret Time (Sec)	Height (μV)	Area ($\mu\text{V}\cdot\text{Sec}$)	Area % (%)	Name
1	FU	46	80	55	4379.0	33370	3.87	Nitrogen
2	FU	80	233	86	59503.0	664567	77.10	Carbon
3	RS	272	717	291	2724.0	164021	19.03	Hydrogen

 8619581 100.00

EAGER 200 Unk Report

Instrument name : Instrument #1 Bline drift (μV):-.7
 Company Name : IVIC Operator Ident. : E.S.
 Sample Ident. : 32 MEB-43 Filename : ag30506
 Sample Weight : 2.053 Calc.method: using 'K. Factors'

Pk. (#)	Ret Time (Sec)	Area ($\mu\text{V}\cdot\text{Sec}$)	Element % (%)	Area Ratio	Name
1	55	33370	3.759	.199153E+02	Nitrogen
2	86	664567	48.799	.100000E+01	Carbon
3	291	164021	4.053	.405172E+01	Hydrogen

Elemental analysis of photoproduct 2:

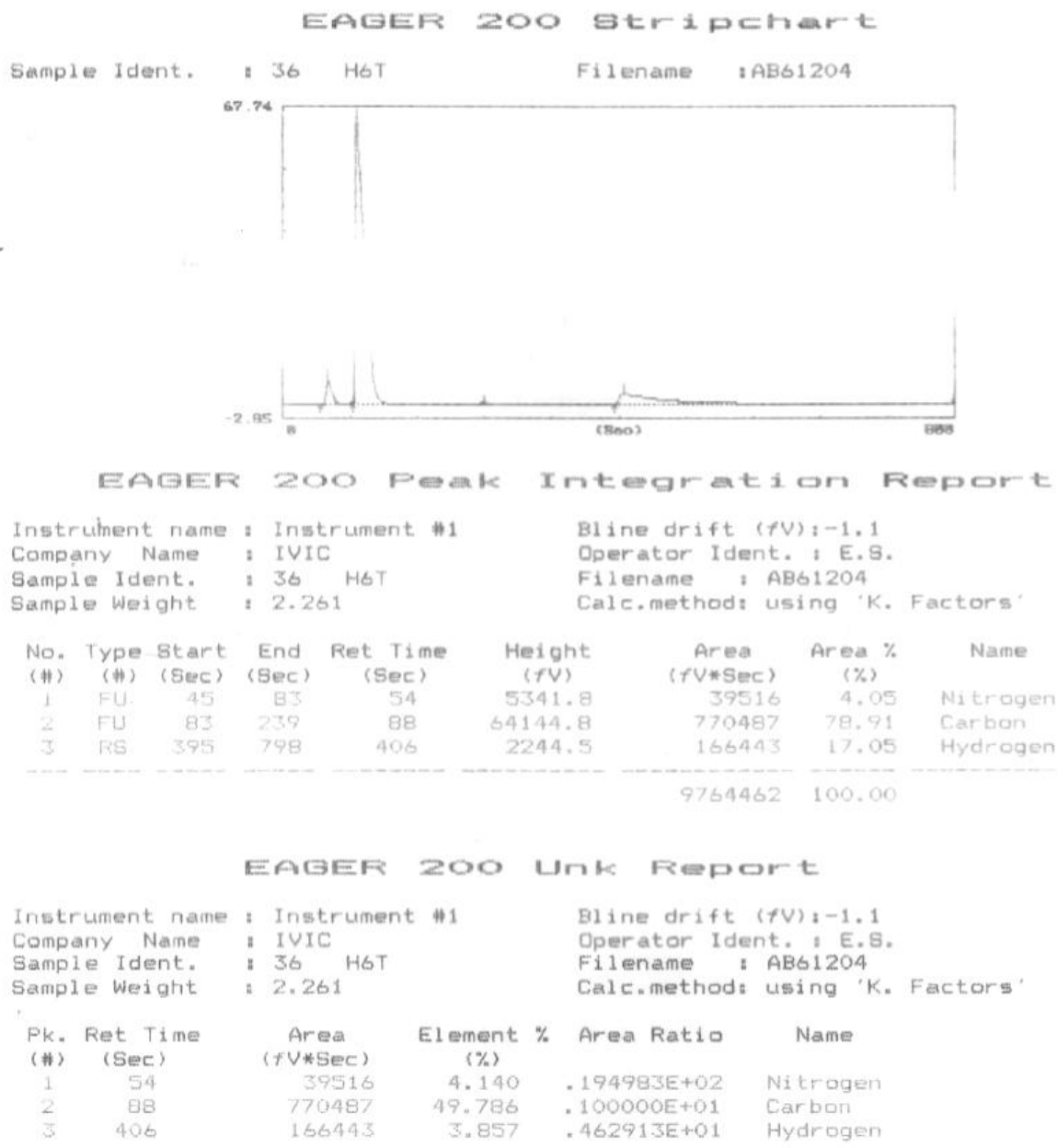


Figure S2. Experimental elemental analysis for co-crystal 1 and compound 2

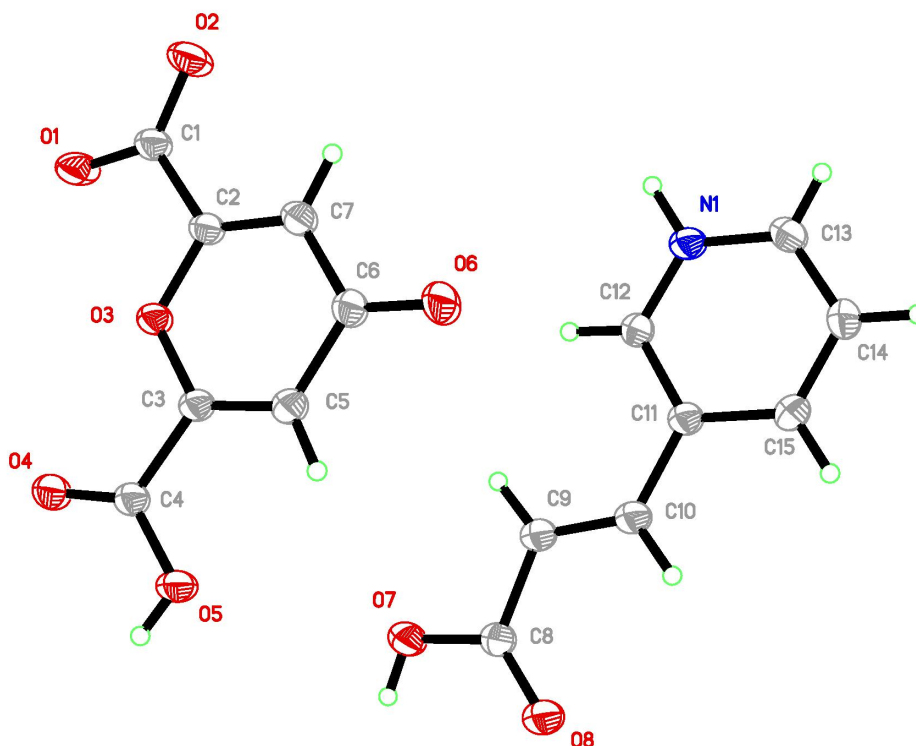


Fig. S3. Thermal ellipsoid representation of the molecular structure of **1** with the applied numbering scheme (50% probability ellipsoids).

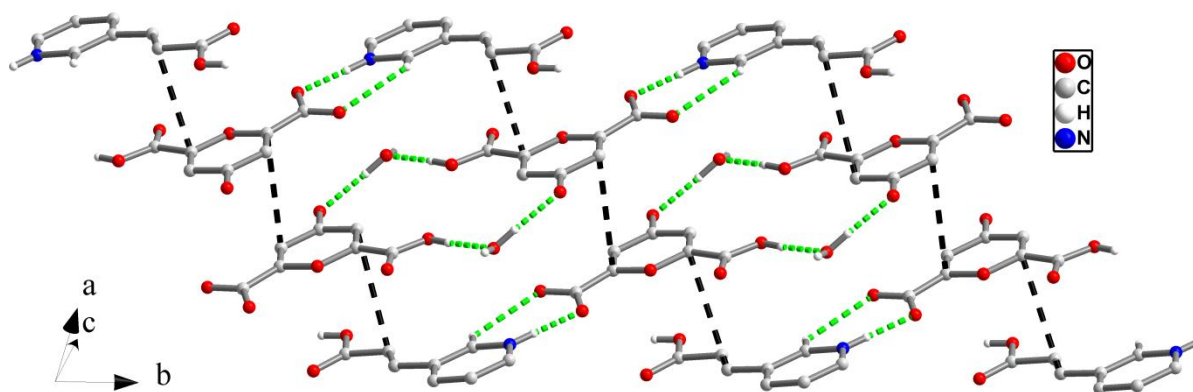
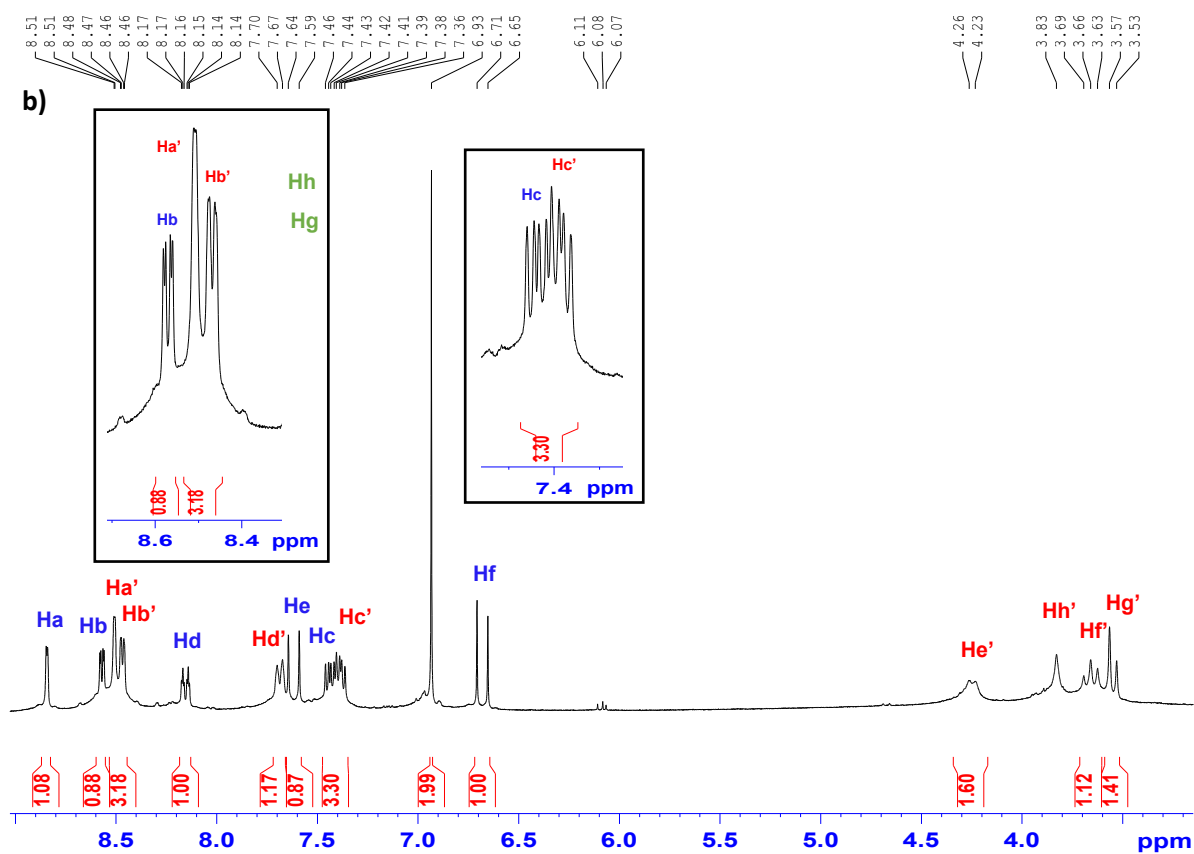
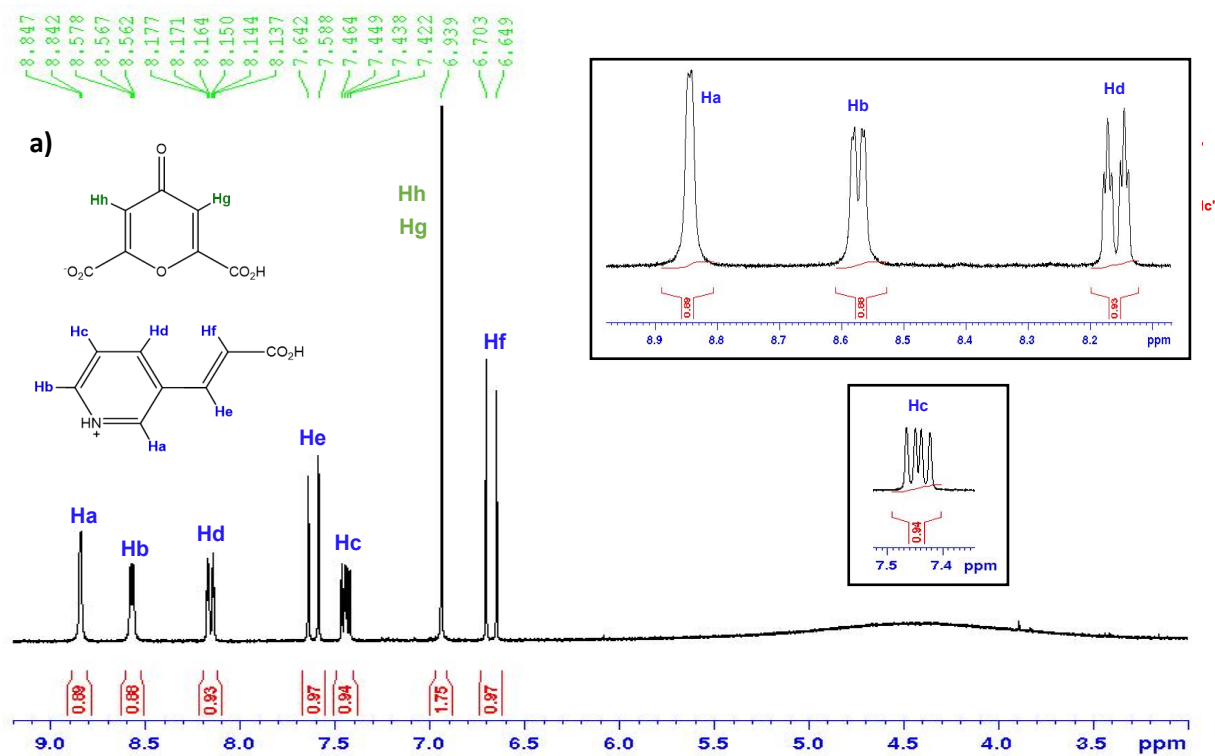


Fig. S4 Packing diagram of co-crystal **1**, showing sequence of ABBA...ABBA layers, green and black dotted lines indicate hydrogen bonds and short π - π interactions, respectively—only O and N bound hydrogen atoms are displayed for clarity; oxygen – red, nitrogen – blue, carbon – grey, hydrogen – light grey).

3.- NMR spectra



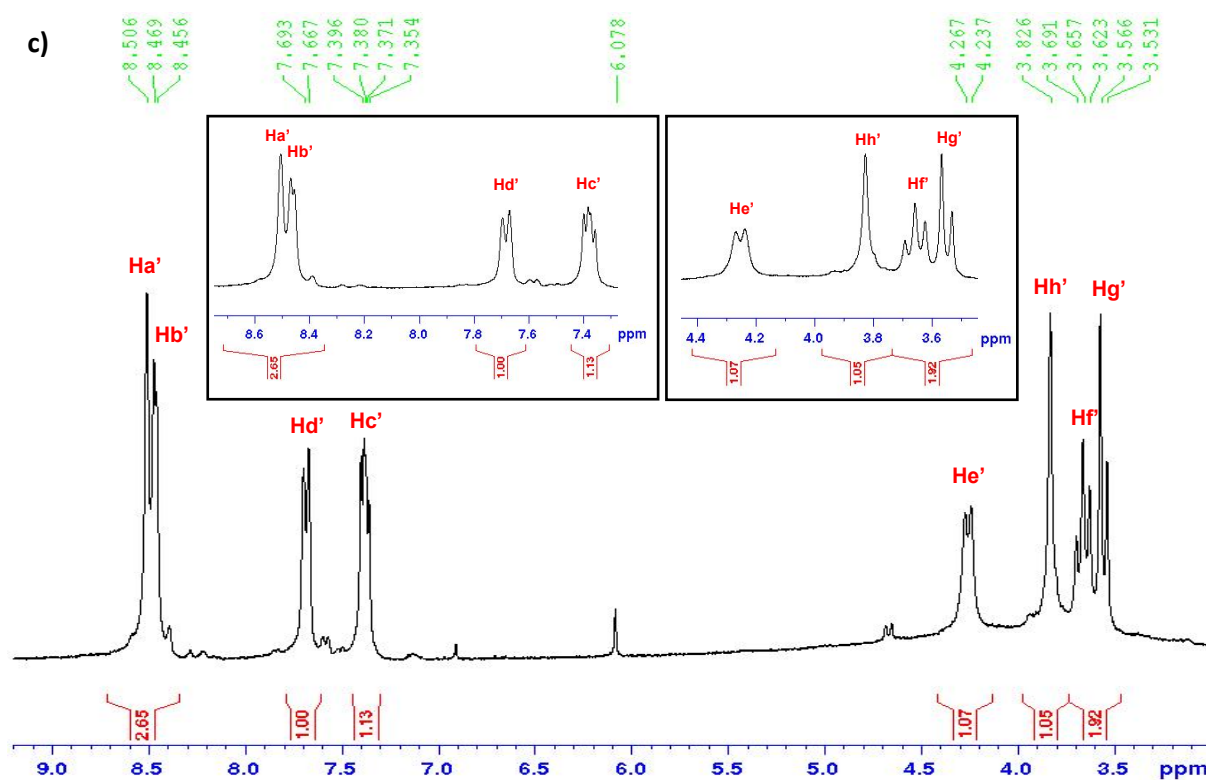


Figure S5. ^1H NMR spectrum in DMSO-d_6 of assembly **1** (a) before irradiation and (b) after irradiation at 350 nm for 72 h. (c) Isolated photoproduct **2**.

4.- FT-IR spectra

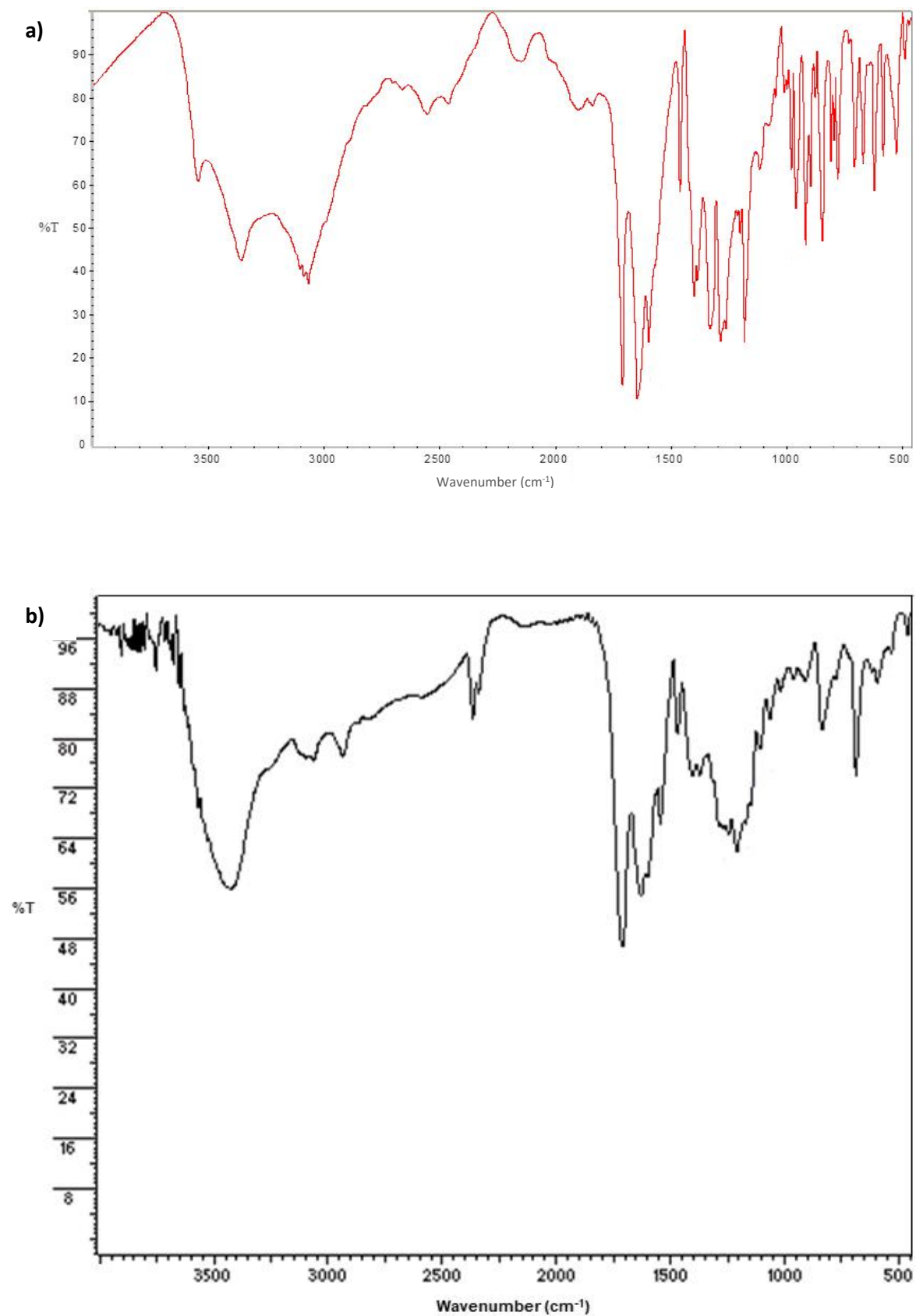


Figure S6. IR spectrum of (a) assembly **1** and (b) photoproduct **2**.

5.- ESI-MASS spectrum

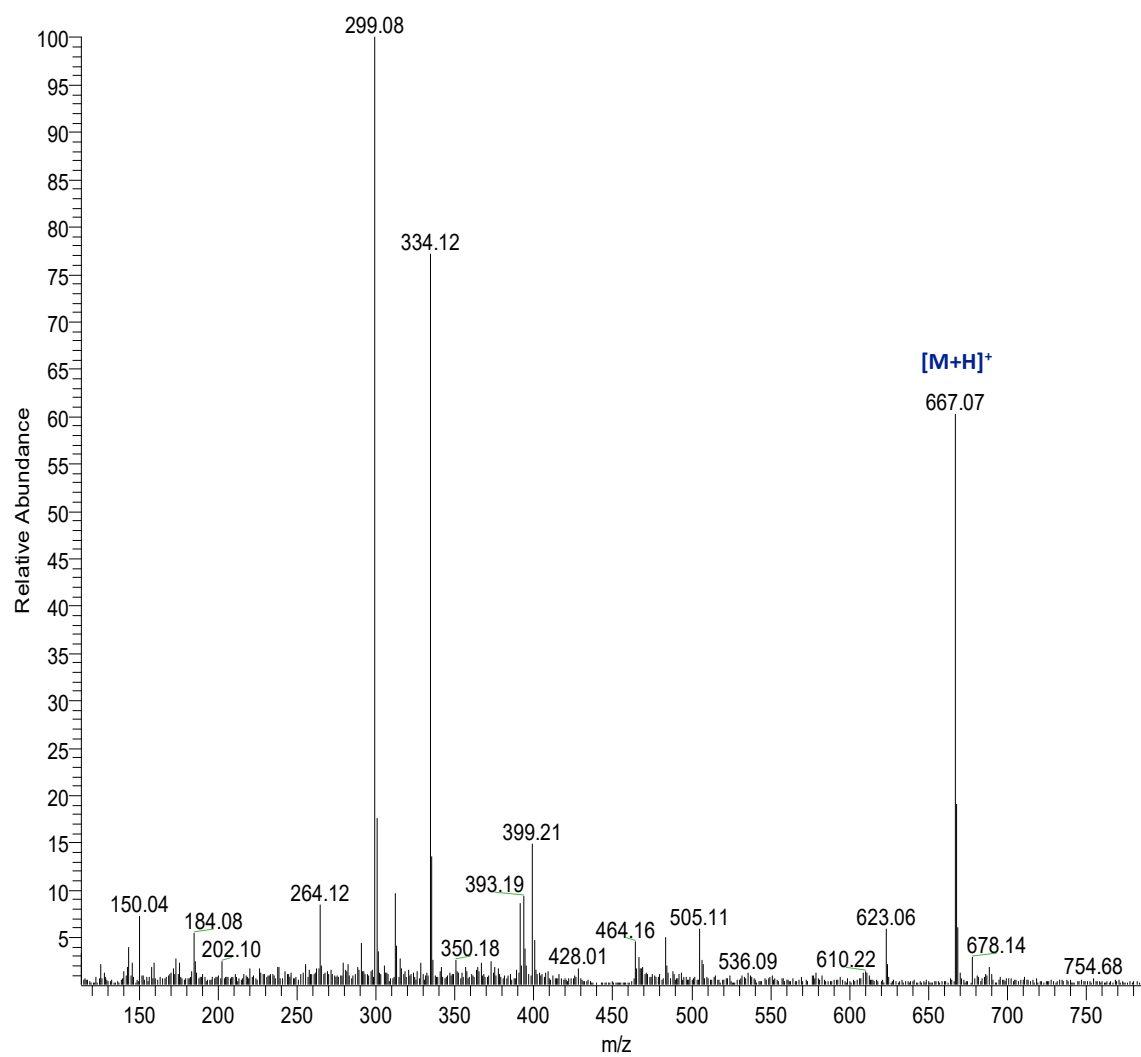


Figure S7. Mass spectrum of photoproduct 2.

6. Crystal structures

General

CCDC 2257007 (for **1**) and CCDC 2252469 (for **2** · 6 DMSO) contain the supplementary crystallographic data for this paper. This data can be obtained free of charge *via* <http://www.ccdc.cam.ac.uk/products/csd/request/> (or from Cambridge Crystallographic Data Centre, 12 Union Road, Cambridge, CB2 1EZ, UK (fax: ++44-1223-336-033; e-mail: deposit@ccdc.cam.ac.uk).

Intensity data were recorded on a Rigaku XtaLAB P200 diffractometer equipped with a Pilatus 200 K detector and SHINE (curved graphite monochromator) optics and Cu K α radiation ($\lambda = 1.54184 \text{ \AA}$) at room temperature (for **1**) and on a Bruker Kappa APEX2 ImuS Duo diffractometer using MoK α radiation ($\lambda = 0.71073 \text{ \AA}$) and QUAZAR focussing Montel optics at -173°C (for **2**). An empirical absorption correction (multi-scan) was applied using the package CrysAlis Pro¹ (for **1**) and SADABS² (for **2**). The structures were solved by direct methods (SHELX XT 2014/5)³ and refined on F^2 using SHELXL 2018/3.⁴ The distances and bond angles, torsion angles, molecular planes, hydrogen bond interactions, among others, were calculated using the PLATON program v1.17.⁵ The graphic representation was made using the Diamond v3.2 program.⁶ All non-hydrogen atoms were refined with anisotropic displacement parameters. For **2** · 6 DMSO the positions of the oxygen and nitrogen bound hydrogen atoms were taken from a difference Fourier map. All other hydrogen atoms were placed in positions of optimized geometry. The isotropic displacement parameters of all H atoms were tied to those of their corresponding carrier atoms by a factor of 1.2 or 1.5. In the crystal structure of **2** · 6 DMSO (dimethyl sulfoxide) the molecule of **2** was located on a crystallographic inversion centre and, consequently, possesses crystallographically imposed C_i molecular symmetry. Crystallographic data, data collection and refinement details for **1** and **2** · 6 DMSO are summarized in Table S1.

Table S1. Crystallographic data, data collection and refinement details for **1** and **2** · 6 DMSO.

	1	2 · 6 DMSO
CCDC no.	2257007	2252469
empirical formula	C ₇ H ₃ O ₆ · C ₈ H ₈ NO ₂ · 2(H ₂ O)	C ₃₀ H ₂₂ N ₂ O ₁₆ · 6 (C ₂ H ₆ OS)
<i>M</i> [g mol ⁻¹]	369.28	1135.26
crystal size [mm]	0.10 x 0.30 x 0.50	0.23 x 0.05 x 0.05
temperature [K]	293	100
crystal system	triclinic	monoclinic
space group (no. Int. Tables)	P-1	<i>P</i> 2 ₁ / <i>c</i> (14)
<i>a</i> [Å]	7.4691(2)	10.0803(11)
<i>b</i> [Å]	10.2107(2)	19.8625(19)
<i>c</i> [Å]	11.3913(2)	14.0812(14)
α [°]	71.336(2)	90
β [°]	78.812(2)	110.710(3)
γ [°]	77.041(2)	90
<i>V</i> [Å ³]	795.04(3)	2637.2(5)
<i>Z</i>	2	2
μ [mm ⁻¹]	1.150	0.339
<i>F</i> (000)	384	1192
abs. corr.	Multi scan	SADABS
<i>T</i> _{min} ; <i>T</i> _{max}	0.731; 1.000	0.713; 0.746
2 θ -range [°]	4.1 ≤ 2 θ ≤ 74.5	3.7 ≤ 2 θ ≤ 54.4
coll. refl.	7565	72015
indep. refl.	3118	5843
obs. refl. <i>F</i> ₀ ≥ 4.0 σ (<i>F</i>)	2891	4586
no. ref. param.	247	334
<i>wR</i> ₂	0.1055	0.0981
<i>R</i> ₁ (<i>F</i> ₀ ≥ 4.0 σ (<i>F</i>))	0.0369	0.0402
Goof <i>F</i> ²	1.06	1.045
7565, 3118, 0.015	7565, 3118, 0.015	7565, 3118, 0.015

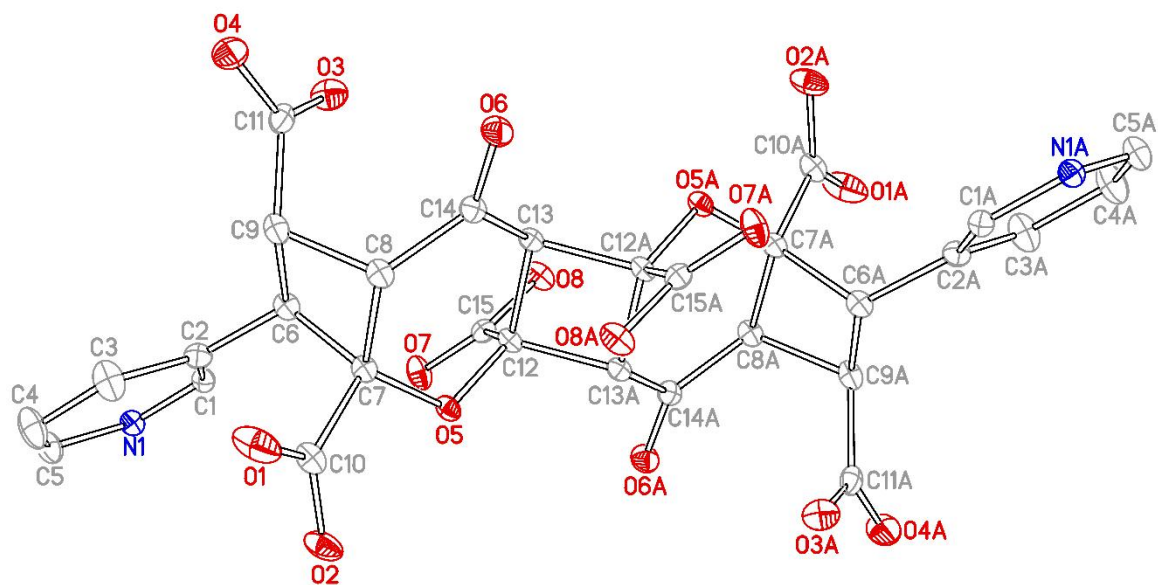


Fig. S8. Thermal ellipsoid representation of the molecular structure of **2** in crystals of **2** · 6 DMSO with the applied numbering scheme (50% probability ellipsoids, hydrogen atoms omitted for clarity).

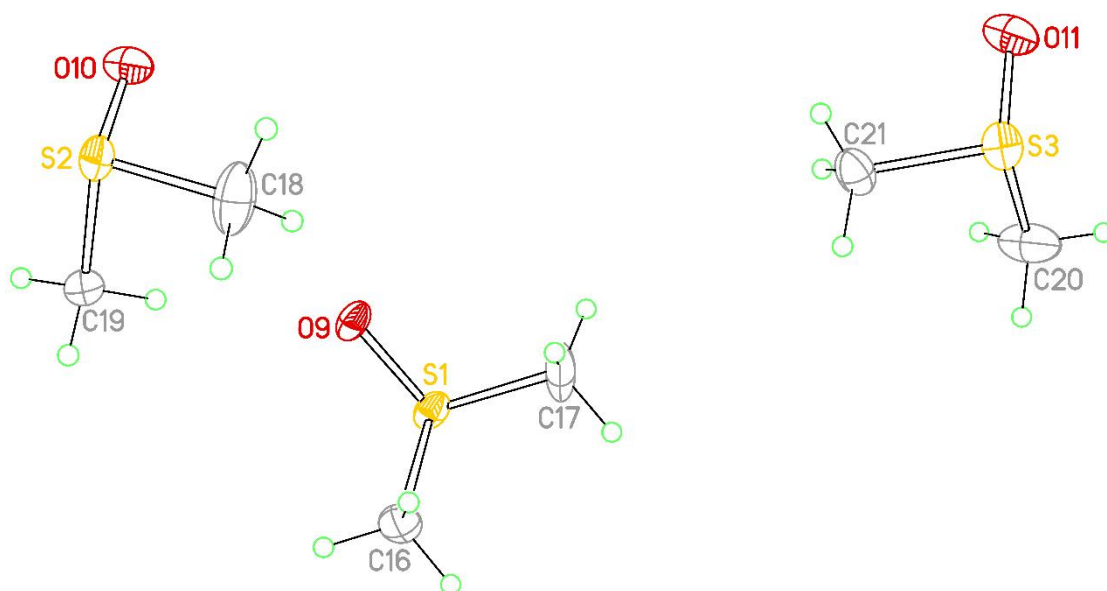


Fig. S9. Thermal ellipsoid representation of the molecular structures of the three independent DMSO molecules in crystals of **2** · 6 DMSO with the applied numbering scheme (50% probability ellipsoids).

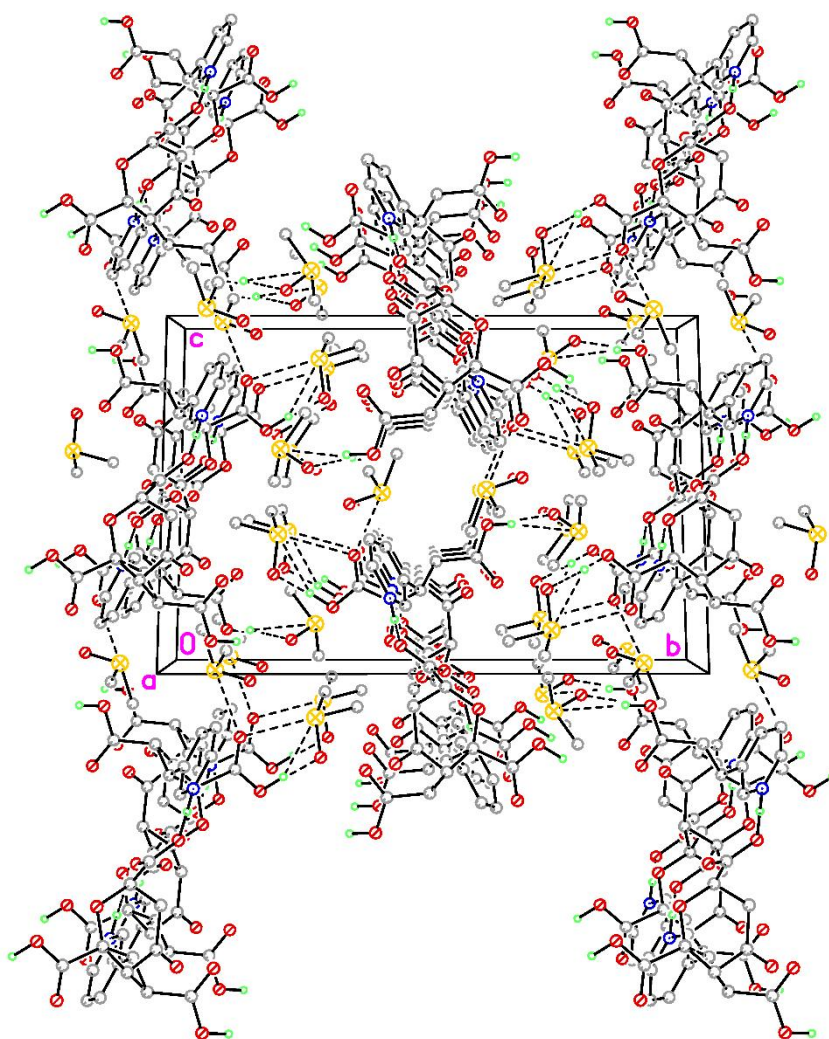


Fig. S10. Packing diagram of $2 \cdot 6$ DMSO (view along the crystallographic *a* axis, dotted lines indicate hydrogen bonds, only O and N bound hydrogen atoms are displayed for clarity; sulphur – yellow, oxygen – red, nitrogen – blue, carbon – grey, hydrogen – light green).

7. Biophysical-Computational characterization

The binding constant K from the binding free energy was calculated as described [25] from the following equation:

$$K = e^{-(\Delta G/RT)} \quad (\text{eq.1})$$

And the inhibition constant for binding of ligand to proteins (K_i) (in units of M) was obtained as,

$$K_i = K^{-1} = e^{(\Delta G/RT)} \quad (\text{eq.2})$$

where, ΔG is binding affinity (kcal/mol), R is the universal gas constant (1.987 cal/K mol), T is the absolute temperature (298.15 K). The equation states that the higher the K_i value, the weaker the binding of the inhibitor to the protein, and, therefore, the protein-inhibitor complex dissociates more easily.

The stability of the Spike-ACE2 complex was analysed by molecular dynamics (MD). Simulations for a docking hit were performed for two purposes: 1) to study the relative stability of the ligand residing in the binding pocket; and 2) sampling of the minimum energy conformations to calculate the perturbation of the thermodynamic and structural stability of the complexes. For a protein-ligand complex, the MD system relaxed first through a series of minimization procedures that includes three phases: relaxation, balance and sampling, as recommended. The MD simulation of the crystal structures was carried out in an explicit water system. Specifically, the solvation of the system was carried out in a solvation box of 8 Å. Our MD system also consisted of one copy of each protein system and one copy of the docking ligand. An Amber99SB-ILDN force field was applied to the complex, with TIP3P water model. The whole system was finally neutralized. Water molecules were treated as rigid bodies in all models, allowing a simulation time interval of 2 fs. Periodic boundary conditions were applied, and Berendsen's algorithm for temperature and pressure docking was adopted. After a first steepest descent (5000 steps) and conjugated gradient (5000 steps) of energy

minimizations with positional restraints on the solute, an initial 100 ps simulation was carried out with the positions of the solute atoms restrained by a force constant of 10 kcal.mol⁻¹ Å⁻² to let the water diffuse around the molecule and for equilibration. The method PME was used to calculate the electrostatic contribution to nonbonded interactions with a cutoff of 14 Å and a time step of 1 fs. The cutoff distance of the van der Waals interaction was 14 Å. After this equilibration run, the NVT (particle numbers, volume, temperature) production run at 300 K was performed with the cell size remaining the same. The SHAKE algorithm was applied to the system, and the time step was set to 2 fs. Ten structures were obtained every 10 ns as target structures extracted from a 100 ns trajectory. For the Root Mean Square Deviations (RMSD) calculations, the equation,

$$RMSD = \sqrt{\frac{1}{n} \sum_{i=1}^n \delta_i^2} \quad (\text{eq.3})$$

where δ_i is the distance between atom i and either a reference structure or the mean position of the n equivalent atoms. All MD simulations and additional adjustments were performed using COSGENE/myPresto. To predict the effect of the stable bond between the compound **2** and the Spike, the minimum energy structures obtained after MD were analyzed using the elastic network models (ENM) frustratometer (<http://frustratometer.qb.fcen.uba.ar/>) and SPECTRUS (<http://spectrus.sissa.it/>). These were used for the prediction of structural deformability in terms of configurational energy frustration and distribution of rigid regions, respectively.

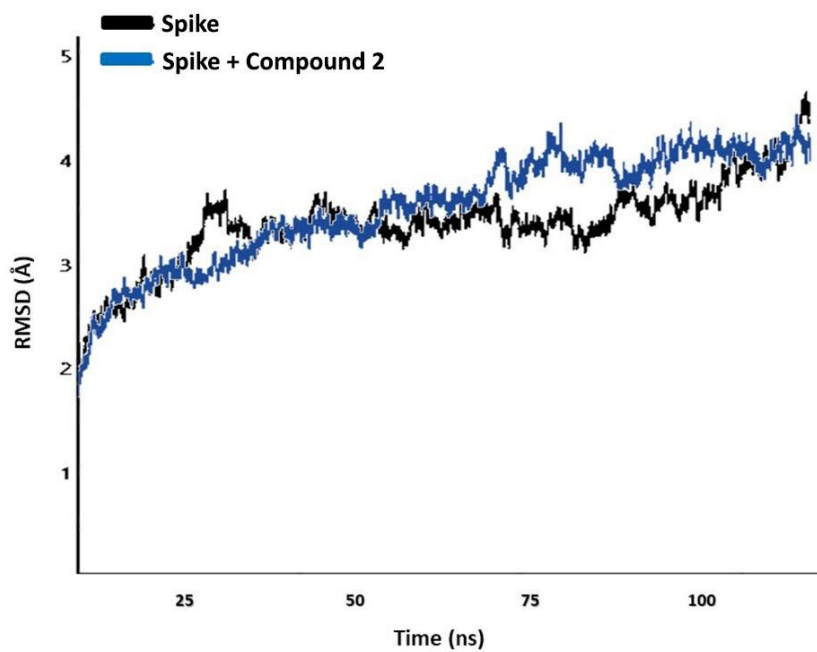


Figure S11.- The root means square deviations (RMSD) performed with COSGENE/myPresto at 100 ns simulation.

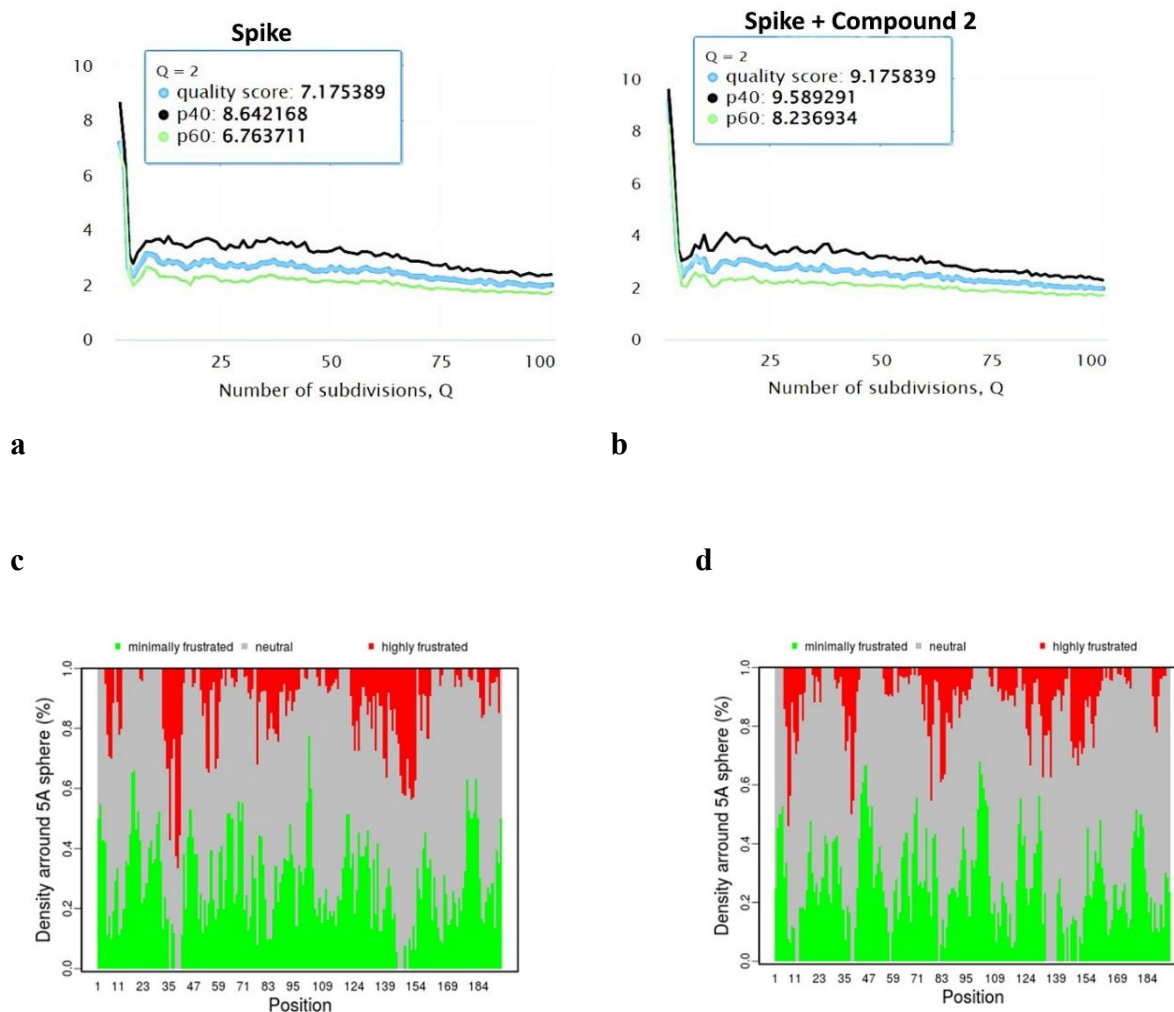


Figure S12.- Diagram of the system stiffness predicted with the elastic network model (ENM) SPECTRUS (<http://spectrum.sissa.it/>) in free protein a) and with the tetramer b), and frustratometer (<http://frustratometer.qb.fcen.uba.ar/>) in free protein c) and with compound 2 d). In frustratometer, the distribution of rigid regions (black curve) and the structural deformability in terms of configurational energy frustration (red bars “unstable region” and green bars “stable region” of the upper right panel) are shown, respectively.

References

- [1] Rigaku Oxford Diffraction. *CrysAlisPro Software system*, Ver. 1.171.40.61a; Rigaku Corporation: Oxford, UK, **2019**.
- [2] L. Krause, Herbst-Irmer, Regine. Sheldrick, George M., Stalke, Dietmar, *J. Appl. Crystallogr.* **2015**, *48*, 3-10.
- [3] G. M. Sheldrick, *Acta Crystallogr., Section A, Foundations and advances.* **2015**, *71*, 3-8.
- [4] G. M. Sheldrick, A short history of SHELX. *Acta Crystallogr., Section A, Foundations of crystallography.* **2008**, *64* (Pt 1), 112–122.
- [5] Spek, A. L. Structure validation in chemical crystallography. *Acta Crystallogr., Sect. D: Biol. Crystallogr.* 2009, *65*, 148–55.
- [6] Brandenburg, K. DIAMOND, Ver. 3.0; Crystal Impact GbR: Bonn, Germany, 1999.